Submillimeter Observations of an Isolated Massive Dense Core

H. Shinnaga[1], T.G.Phillips[1,2], R.S. Furuya[2,3], R. Cesaroni[4],
[1] **Caltech Submillimeter Observatory**, [2] Caltech, [3] NAOJ, Japan, [4] Osservatorio Astrofisico di Arcetri, INAF, Italy

Abstract

Submillimeter continuum (350- and 450-μm) and line emission of an isolated massive dense core have obtained using the CSO 10.4 meter telescope. The core hosts an early B-type massive (proto)star, IRAS 20126+4104. The radial density profile of the core indicates that the inner region of r < 0.1 pc may experience infall, while the wave of infall has not reached yet at the outer region of r > 0.1 pc. From the flux ratio map made from the two submillimeter bands, following complex structures are revealed: (1) a bipolar feature that coincides with the molecular outflow, (2) a cocoon of cold dense core with warm surface, and (3) cold layer outside of the cocoon. The bipolar feature may trace cavities inside of the bipolar outflow. CO J = 6─5 observations revealed narrow line width quiescent molecular components in the envelope that shows velocity gradient of ~ 2 km $s^{-1}pc^{-1}$, probably due to rotation, from east to west. The core mass is estimated to be ~ 200 M . The rotation axis of the envelope over a 1 pc scale is almost opposite sense of that of the disk like feature with a scale of ~0.06 pc associated with the (proto)star. Emissivity spectral index and temperature of the dust emission are estimated to be ~1.7 and ~ 40 K, respectively. Eighteen clumps are identified in the CO 1─0 data taken with the Owens Valley Millimeter Array. Most of the clumps show 350 μm flux enhancement on the locations, suggesting that these clumps are real physical entities, maybe created through fragmentation processes. The measured clump mass distribution is ΔN/ΔM ∝ M^(−1.6±0.4) over a range of 0.01 M to 40 M . The shallow slope might indicate that the clumps are formed due to pure gravitational contraction without significant turbulent support, as the contributions from non-thermal components at the outer region of the massive dense core are measured not to be significant.

Introduction

Understanding massive star formation and the evolution is an important subject in the field of astrophysics. We identified an isolated massive dense core in an early phase of massive star formation with a simple configuration and carried out a detail observational study on the dense core. The massive dense core hosts an early B type massive (proto)star, IRAS 20126+4104. Some highlights of the study are presented. The study was mainly done using the 10.4 meter telescope at the Caltech Submillimeter Observatory (CSO).

Observations

Table 1. Observations

Emission	Center frequency (GHz)	Bandwidth (MHz)	Telescope/ Instrument	beam size (″)	FOV ($arcmin^2$)	LAS[a] (″)	Velocity resolution (kms^{-1})	Reference
350μm continuum	849.4	102900	CSO/SHARC II	8.7	9 × 9	...	...	This work
450μm continuum	658.3	67900	CSO/SHARC II	9.8	9 × 9	...	...	This work
CO $J = 6-5$	691.473076	50	CSO/690GHz Rx	10	3 × 2.7	...	0.6	This work
CO $J = 7-6$	806.651776	250/1000	HHT[b] /800GHz Rx	10	...	...	0.9	Kawamura et al. (1999)
CO $J = 1-0$	115.271204	1000	OVRO-MMA/230GHz Rx	7.53×7.09	3 × 3	16	1.3	Shepherd et al. (2000)

[a]The largest angular scale detected with the interferometric observation.

[b]The Heinrich Hertz Telescope.

Overall Structures

About a field of 9′ centered on the object IRAS 20126+4104 was mapped at the wavelength of 350μm and 450μm with the SHARC II. The mapping observation confirmed that this is the only prominent dense core existing within the 4 pc area centered at the position of the (proto)star, indicating that the core is an isolated dense core in the region.

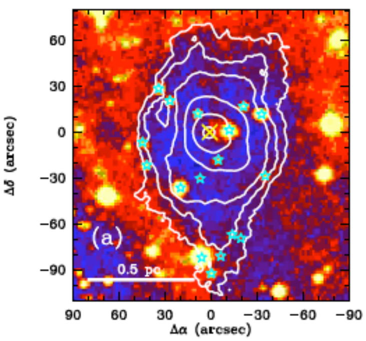

FIG 1. SHARC II 350μm dense core images (contours) overlaid on the optical image (DSS, 0.5μm, color). Blue stars mark the positions of foreground stars.

Radial Distribution

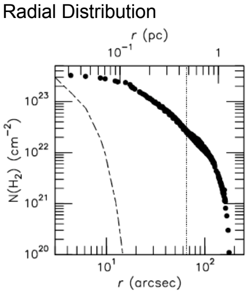

FIG 2. Column density distribution of the dense core.

Inner part of the dust core has a flatter power-low index compared to that of outer part. The power low of volume density at radius between 0.03 and 0.13 pc is r^(−1.26±0.03). The volume density in ranges of radius between 0.13 and 0.3 pc decreases with r^(−2.32±0.02). The slope index −1.26 at r ≤ 0.1 pc is somewhat similar to the density profile for a free-fall region of ρ(r) ∝ r^(−3/2), predicted by the Larson-Penston model (Larson 1969; Penston 1969) and the Shu's model (Shu et al. 1987). The slope index −2.32 for a radius range between 0.1 and 0.3 pc is similar to the density profile ρ(r) ∝ r−2, for a system under hydrostatic equilibrium. These two distinct power low indices of the density profile may indicate that the inner region of r < 0.1 pc experiences infall while the wave of infall has not reached yet at the outer region of r > 0.1 pc.

Quiescent Rotating Massive Dense Core

Assuming the velocity shift is caused by rotation of the core and the centrifugal force balances with the gravity, estimated mass of the molecular dense core is ~ 200 M. The measured velocity gradient is 2 $kms^{-1}pc^{-1}$. Assuming the rotational energy balances with the gravity, the enclosed mass of the core is estimated to be about 200 $M_{\odot}$. The rotation axis of the molecular warm dense gas component is almost opposite sense of the rotation axis of the disk like structure associated with the (proto)star.

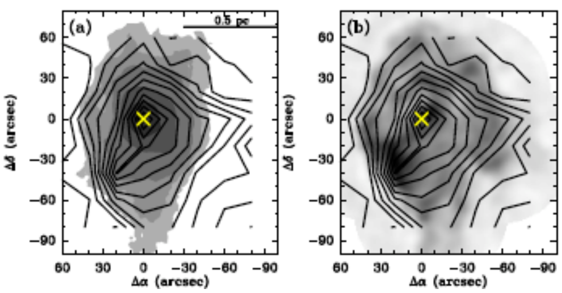

FIG 4. Comparison of CO J = 6 ─ 5 ambient components (contours, $|V_{LSR} - V_{CO6-5}|$ < 2.5 kms−1) with (a) 350μm dust continuum and (b) CO 1─0 ambient components (both in gray scale). The CO contours are drawn from 2 σ with 2 σ spacing.

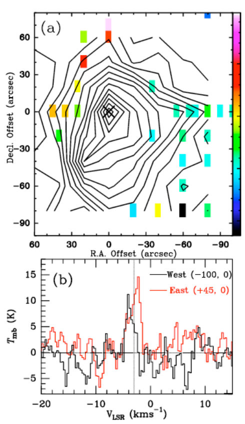

FIG 5. (a) The LSR velocity of the quiescent gas overlaid on the CO 6-5 ambient components (contours). Diagram (b) shows CO 6─5 spectra observed in east (+45", 0) and west (+100", 0) positions relative to the 1mm/3mm continuum peak. Dotted vertical line is drawn at the CO 6 ─ 5 center velocity.

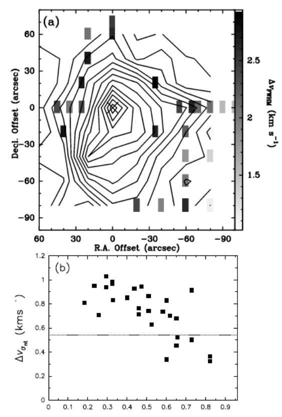

FIG 6. (a) Velocity width of the CO 6─5 quiescent gas components overlaid on the CO 6-5 ambient components (contours). Diagram (b) shows the non-thermal velocity dispersion of the components. Horizontal dotted line shows the kinetic velocity dispersion at 40 K.

Fragmentation: Clumps and the Mass Spectrum

Good spatial correlation is found between the submillimeter dust peaks and the CO 1 ─ 0 ambient components. One can identify quite a few peaks of molecular clumps, as numbered in the two diagrams. For those clumps with numbers, except for 13 and 16, 350μm SHARC II dust map shows flux enhancement at the same locations as the clump locations. This strongly indicates that these clumpy molecular components are real physical entities, most likely created through fragmentation process, rather than due to local chemical abundance variation or chemical inhomogeneities.

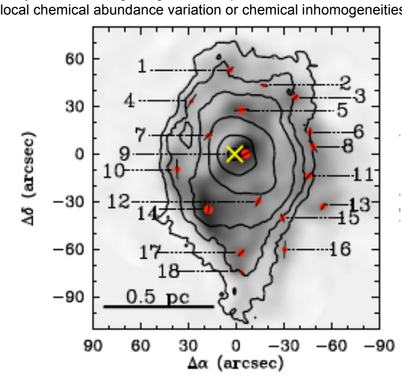

FIG 9. Overlay of the 350μm images (contours) on the ambient gas components taken with the OVRO-MMA. The filled circles represent the locations of the clumps. The area of the circle is proportional to the intensity of each clump. Black solid lines drawn on each clump are major axes of the clumps.

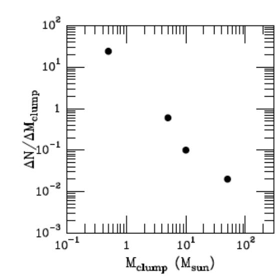

FIG 10. The clump mass spectrum.

350micron/450 micron Flux Ratio Map

There are two parameters that change the flux ratio, namely, emissivity spectral index, and temperature of dust grains T_{dust}. To achieve higher flux ratio values, both temperature and spectral index need to be high. When T = 40 K, spectral index of 1 and 2 correspond to the flux ratios of 1.9 and 2.4, respectively. When =1.7, temperature of 20, 40, 60 K matches with flux ratio of 1.9, 2.3, and 2.4, respectively. One cannot distinguish contribution from emissivity and from the temperature. There are three major components in the ratio map, namely (1) bipolar feature at the center of the core, (2) ~ 0.5 pc diameter elongated component whose edge show high ratio value (~ 3), and (3) lower ratio components outside of the component (2). The ratio value inside of the bipolar lobes is ~ 2. The bipolar structure is situated in the component (2). Outside of (2), there are components whose flux ratio values are relatively lower, <~ 2.

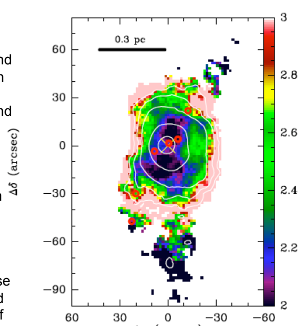

FIG3. Flux ratio map made from 350 and 450 μm images. White contours show the 450 μm image drawn at 3 , 5 , 9 , 27 , and 81 σ. A yellow cross and red circles represent the 3mm/1mm millimeter continuum peak and the locations of molecular hydrogen knots, respectively.

Molecular Bipolar Outflow

The red-shifted bipolar outflow lobe is much more extended (about more than twice) compared with the blue-shifted outflow lobe. This might be related to the fact that there is third massive molecular clump located at the northern edge of the blue outflow lobe. At the north edge of the blue shifted outflow component, one can identify the shocked H2 knot, H2-1. The knot might be caused by the collision between blue-shifted outflow and the dense molecular clump located at the northern edge of the lobe. The strong correlation between CO 6─5 peaks and shocked H2 knots indicate they are physically associated. From the outflow velocity and the extension of the outflow, one can estimate the dynamical age of bipolar outflow. The estimated age of the outflow is about ≥17000 years.

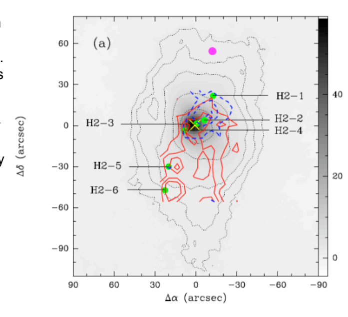

FIG 7. CO J = 6─5 blue-shifted (blue dashed contours) and red-shifted (red solid contours) emission superposed on 350μm dust continuum emission. The yellow cross at the center marks the location of the 1mm/3mm peak. Green dots and a purple dot represent the locations of shocked H2 knots and H /[SII] knot (Shepherd et al.2000), respectively.

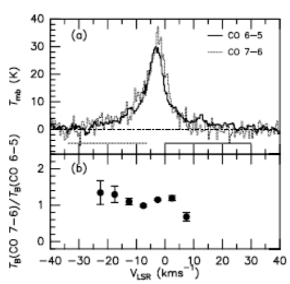

FIG 8. (a) CO 6 ─ 5 (this work) and 7 ─ 6 (Kawamura et al. 1999) spectra observed towards the position of the mm continuum. Note that CO 7─6 spectrum has a lower limit of the temperature scale. (b) Ratio of brightness temperatures of CO 7-6 and 6-5 transitions.